been estimated to be about 1.5% that of the strong line. This intensity is consistent with about a 3% impurity of Zr^{95} in the sample. Another well-known gamma ray[6] from the decay of Zr^{95} has an energy of 760 keV and its intensity is about 80% of that of the 726-keV gamma ray. Its presence is suggested by a slight hump on the low-energy side of the line from the decay of Nb^{95}. It is clear from the figures that no gamma ray of any appreciable intensity is present in the spectrum near 753 keV. It has been estimated that such a gamma ray would have been detected if its intensity were $\geq \frac{1}{2}\%$ of that of the strong line at 765.8 keV.

The spectrometer was calibrated by observing the gamma ray[7] at 661.595±0.076 keV from Cs^{137} (Fig. 2) and the Co^{60} lines[8] at 1173.13±0.15 keV and 1332.34 ±0.15 keV. For the energy determination, the composite spectrum from the standards and unknown was recorded with all the sources in place near the detector to minimize the effects of shifts in gain caused by variations in counting rates. It is estimated that the peak positions are determined to about 0.2 channel. Deviations from linearity in the system produce an uncertainty in the position of the line of 764.2 keV of about one-tenth of the error assigned. These measurements yield a value of 765.8±0.4 keV for the energy of the gamma ray that follows the beta decay of Nb^{95}.

[7] R. L. Graham, G. T. Ewan, and J. S. Geiger, Nucl. Instr. Methods **9**, 245 (1960).

[8] G. Murray, R. L. Graham, and J. S. Geiger, Bull. Am. Phys. Soc. **7**, 81 (1962).

PHYSICAL REVIEW VOLUME 142, NUMBER FEBRUARY 1966

Photofission of U^{238} Induced by 17.5-MeV Monoenergetic Gamma Rays*†

J. L. Meason and P. K. Kuroda
Department of Chemistry, University of Arkansas, Fayetteville, Arkansas
(Received 11 May 1965; revised manuscript received 11 October 1965)

Fission yields were determined radiochemically using low-level counting techniques for fourteen mass chains from photofission of U^{238} induced by 17.5-MeV monoenergetic gamma rays from the $Li^7(p,\gamma)2He^4$ reaction. Fine structure in the mass-yield curve in the region $A=131$-135 was observed, with the peak occurring at $A=132$. A striking similarity was noted between the photofission mass-yield curve in the mass-130-136 region and the relative abundance pattern of the excess fission xenon recently observed in certain meteorites.

I. INTRODUCTION

SEVERAL workers have studied the mass distribution in photofission of uranium.[1–6] However, the previous studies were limited to the fission caused by bremsstrahlung beams and the photofission mass yields for uranium irradiated with monoenergetic gamma rays have never been reported. In this work, we utilized the 17.5-MeV gamma rays from the $Li^7(p,\gamma)2He^4$ reaction to study the mass distribution, especially fine structure in the region $A=131$–135, in the photofission of U^{238}.

The University of Arkansas 400-kV Cockcroft-Walton Accelerator[7] is normally operated for the production of 14.8-MeV neutrons using the well-known $T(d,n)He^4$ reaction. For the experimental work reported here, the accelerator was modified so that the $Li^7(p,\gamma)2He^4$ reaction could be utilized as a source of 17.5-MeV gamma rays. The gamma-ray flux thus available was rather low (of the order of 10^6 γ/cm^2 sec) and low-level radiochemical and counting techniques had to be employed. As an example of the counting rate observed in a typical experiment, only 4 counts per minute of 8.1-day I^{131} were observed for a 2-h irradiation of about 2 g of U_3O_8. Nevertheless, it was possible to measure the yields of short-lived fission products belonging to 14 mass chains and to obtain the general shape of the mass-yield curve. The yields for five consecutive mass numbers, 131 to 135, have been measured by isolating the short-lived iodine isotopes at

* This work was supported by the U. S. Atomic Energy Commission.

† This paper represents a part of the dissertation submitted by J. L. Meason to the Graduate School of the University of Arkansas in partial fulfillment of the requirements for the degree of Doctor of Philosophy.

[1] R. A. Schmitt and N. Sugarman, Phys. Rev. **95**, 1260 (1954).

[2] H. G. Richter and C. D. Coryell, Phys. Rev. **95**, 1550 (1954).

[3] L. Katz, T. M. Kavanagh, A. G. W. Cameron, E. C. Bailey, and J. W. T. Spinks, Phys. Rev. **99**, 98 (1955).

[4] J. B. Dahl and A. C. Pappas, University of Oslo, Norway, 1955, unpublished data cited in Ref. 6.

[5] R. W. Spence, unpublished results cited in J. M. Blatt and V. F. Weisskopf, *Theoretical Nuclear Physics* (John Wiley & Sons, Inc., New York, 1952), Chap. 5.

[6] R. B. Duffield, R. A. Schmitt, and R. A. Sharp, in *Proceedings of the Second United Nations Conference on the Peaceful Uses of Atomic Energy, Geneva, 1958* (United Nations, Geneva, 1958), Vol. 15, p. 202.

[7] W. L. Bronner, K. E. Ehlers, W. W. Eukel, H. S. Gordon, R. C. Marker, F. Woelker, and R. W. Fink, Nucleonics **17**, 94 (1959).

various time intervals and by analyzing the decay curves into the five components.

II. EXPERIMENTAL

A. Preparation of the Lithium Target

The target was prepared from natural lithium metal in an inert argon atmosphere and was mounted in the beam tube without removal from the argon atmosphere. The lithium metal was removed from the protective xylene solution into the argon atmosphere of the dry box and immersed in about 10 ml of methyl alcohol. The ensuing reaction removes all the lithium oxides, scale, etc., and exposes the fresh metal surface. The piece of lithium metal (about 1 cc) was transferred to a small stainless steel crucible and heated with a hot plate to the melting point (185°C). The melted lithium metal was placed in a 1-in. cupped copper disk that had been previously tinned on the back side with indium solder. The lithium metal was allowed to flow around the copper disc to ensure a good bond between the two metals. It may be of interest to note here that if the temperature of the system exceeds the melting point of lithium by a considerable amount, the lithium metal does not bond to the copper. The lithium target was allowed to cool while the target plate was heated to the melting point of indium solder. When the indium solder melts, the lithium target was placed in position on the target plate, removed from the source of heat and allowed to cool before mounting in the beam tube. After cooling, the target plate was placed in position and evacuated with a fore pump for about 10 min before opening the target area into the main vacuum system.

B. Depleted Uranium

$U^{238}O_3$ was supplied by the U. S. Atomic Energy Commission, Oak Ridge, Tennessee. The isotopic composition determined at Oak Ridge was 99.989% U^{238} and 0.011% U^{235}. This material was received chemically impure and was exhaustively purified.[8] After purification the uranium was converted to the nitrate and was used as such for the subsequent experiments.

The contribution of neutron-induced fission resulting from the (γ,n) reactions and fission itself has been found by Schmitt and Sugarman[1] and Richter and Coryell[2] to be less than 1%. A control experiment was performed in which uranyl nitrate was sandwiched between two aluminum foils and irradiated for a period of 2 h. The aluminum foils monitor the neutron flux [produced by (γ,n) reactions and fission] passing through the sample by the production of Mg^{27} via the $Al^{27}(n,p)Mg^{27}$ reaction. At the end of the irradiation, the aluminum monitors were removed and the 10-min activity of Mg^{27} was counted. The average activity between the front and back aluminum foils was six counts per minute. This activity, compared to that observed for I^{131}, corresponds to a neutron-induced-fission contribution of 1.5%.

C. Radiochemical Procedures

Standard radiochemical procedures have been employed for the isolation and purification of the isotopes of bromine, strontium, molybdenum, ruthenium, silver, iodine, and barium.[9]

Sample sizes ranged from about 8 to 45 g of uranyl-nitrate. Immediately following the irradiation, the target material was dissolved in distilled water and diluted to 100-ml total volume in all but one case in which the entire sample was used for the bromine analysis. Aliquots were taken from this 100-ml solution for the radiochemical analysis of the various fission products. The length of irradiations ranged from 30 min to 2 h. The time interval between the end of the irradiation and the chemical isolation of an element ranged from a few minutes to more than ten days. This arrangement enables one to isolate the short-lived activities before the long-lived activities grown in, or to allow all the short-lived activities to decay so that only the longer lived activities remain.

D. Counters and Counting Techniques

All beta counting was done in CE-14SL Tracerlab Low Background Beta Counters. In some cases the gamma spectra were taken to check the purity of the separation and also to have an independent method for checking the beta counting results.

All samples were mounted by using the filter-stick technique to provide an evenly distributed precipitate over a well-defined area. The samples were counted on a saturation-backscattering thickness of stainless steel ($\frac{1}{2}$ in. thick).

In order to convert observed counting rates to absolute activities, a method for calculating the detection efficiencies may be employed as described at the Conference on Absolute Beta Counting.[10]

This technique was used for those nuclides for which measured self-absorption curves were not available. Since f_{SSA} [f_{SSA}=correction for scattering and self absorption] as given by Nervik and Stevenson[11] varies only ~5% for β's from 0.6- to 2.8-MeV maximum energy at the sample densities employed here, the efficiencies determined in this manner varied little (less than 5%), for the nuclides in question from the self-absorption curves for the long-lived isotopes determined experimentally.

[8] W. W. Scott, in *Standard Methods of Chemical Analysis*, edited by N. H. Furman (D. Van Nostrand Company, Inc., New York, 1939), 5th ed., pp. 1019–1022.

[9] *The Radiochemistry of the Elements*, Nuclear Science Series NAS-NS3104 (National Academy of Sciences–National Research Council, Washington, D. C., 1961).

[10] *Conference on Absolute Beta Counting, No. 8*, Nuclear Science Series (National Academy of Sciences–National Research Council, Washington, D. C., 1950).

[11] W. E. Nervik and P. C. Stevenson, Nucleonics **10**, 18 (1952).

E. Treatment of Data

For each sample the gross beta decay was observed and resolved into the various components using reported half-lives. From a knowledge of the absolute activity at the end of the irradiation, the total number of atoms of a particular species produced during the irradiation was determined by applying a correction for the decay of the species during irradiation.

$$A_{\text{total}}=[A\lambda_A/(1-e^{-\lambda_A t})]t, \quad (1)$$

where A_{total} = total number of atoms of species A produced in the bombardment, $A\lambda_A$ = activity of A at end of bombardment, and t = length of bombardment.

The absolute yield of Ba^{140} was taken to be 6.00%, and all other yields were measured relative to Ba^{140} by means of the equation

$$\text{Yield of } A=\frac{\text{Yield of } Ba^{140}}{(Ba^{140})_{\text{total}}}(A_{\text{total}}). \quad (2)$$

III. RESULTS AND DISCUSSION

The experimental results are shown in Table I and are plotted in Fig. 1. A smooth curve can be drawn through most of the observed points and mirror points, except that the observed point for $A=135$ is abnormally low. We have so far been unable to explain the low observed yield at $A=135$.

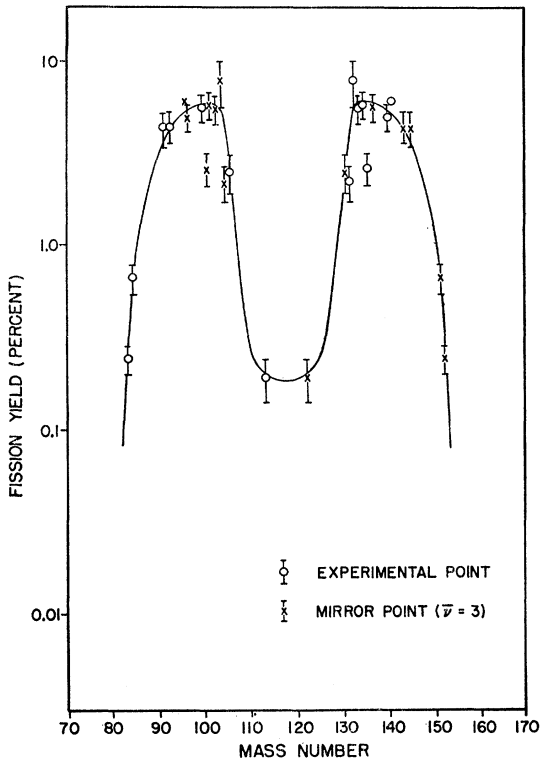

FIG. 1. The mass-yield curve for 17.5-MeV photofission of U^{238}. The mirror points were calculated for $\bar{\nu}=3$.

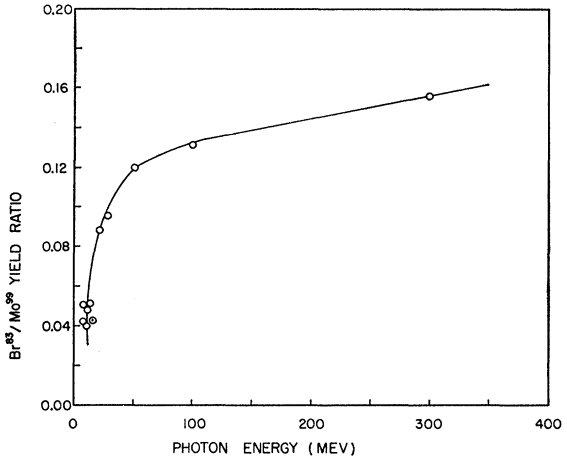

FIG. 2. The Br^{83}/Mo^{99} ratio as a function of photon energies. It shows the change of the general pattern of the photofission mass-yield curves as a function of the photon energy. ○: Data taken from the article by Duffield *et al.* (Ref. 6). ⊙: This work.

Figure 2 shows the variation of Br^{83}/Mo^{99} fission yield ratios as a function of the photon energy. It demonstrates the change of the general pattern of the photofission mass-yield curves as a function of the photon energy, i.e., the trough region fills up and the wings splay out as the photon energy increases.

Aside from the abnormally low yield observed at $A=135$, a "spike" seems to exist at $A=132$, rather than at $A=133$, as shown in Fig. 3. Broom[12,13] has recently observed a fine structure in fast neutron-induced fission of U^{238} and Th^{232}. In the case of U^{238}, the fine structure appears at $A=132$, while in the case of Th^{232} at $A=134$. In both cases, Broom was able to explain the occurrence of fine structure at least qualitatively. The fact that a "spike" is produced at $A=132$ can be demonstrated in

TABLE I. 17.5-MeV photofission chain yields of U^{238} measured in this work.

Nuclide	Percent yield
Br^{83}	0.24±0.04
Br^{84}	0.66±0.12
Sr^{91}	4.3 ±0.9
Sr^{92}	4.4 ±0.9
Mo^{99}	5.6 ±1.0
Ru^{105}	2.5 ±0.6[a]
Ag^{113}	0.19±0.05[a]
I^{131}	2.2 ±0.5
I^{132}	7.8 ±2.2
I^{133}	5.5 ±1.0
I^{134}	5.7 ±1.0
I^{135}	2.6 ±0.5
Ba^{139}	4.9 ±0.8
Ba^{140}	6.00

[a] Data obtained by R. Ganapathy.

[12] K. M. Broom, Phys. Rev. **126**, 627 (1962).
[13] K. M. Broom, Phys. Rev. **133**, B874 (1964).

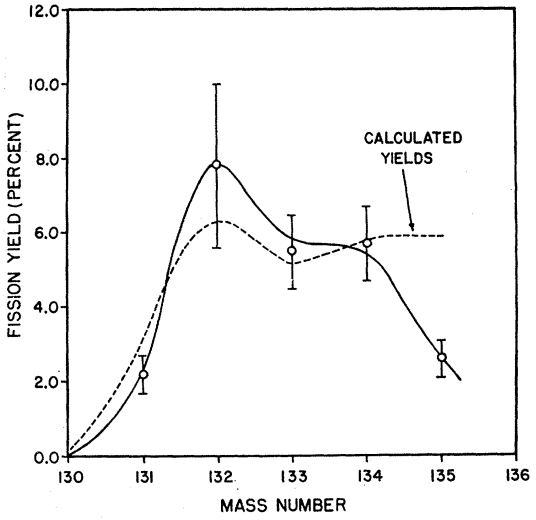

FIG. 3. Fine structure in the region $A=130$–136, ⊼: Measured yields. – – – Mass-yield curve calculated according to the method proposed by Broom (Refs. 12, 13).

the case of U^{238} photofission in essentially the same manner as in the case of the 14-MeV neutron-induced fission of U^{238}.

TABLE II. Independent yields calculated by Pappas' method.[a]

A	Z_p	Z	$Z-Z_p$	Fraction of chain yield	Yield assumed from Fig. 1 (%)	Independent yield
131	50.6	49	−1.60	0.09	3.03	0.27
	50.6	50	−0.60	0.37	3.03	1.11
	50.6	51	0.40	0.42	3.03	1.26
	50.6	52	1.40	0.13	3.03	0.39
	50.6	53	2.40	0.001_5	3.03	···
132	50.97	49	−1.97	0.03	5.57	0.17
	50.97	50	−0.97	0.25	5.57	1.38
	50.97	51	0.03	0.47	5.57	2.59
	50.97	52	1.03	0.24	5.57	1.32
	50.97	53	2.03	0.02	5.57	0.11
133	51.35	50	−1.35	0.15	5.60	0.86
	51.35	51	−0.35	0.40	5.60	2.28
	51.35	52	0.65	0.35	5.60	2.00
	51.35	53	1.65	0.08	5.60	0.46
	51.35	54	2.65	···	5.60	···
134	52.42	51	−1.42	0.14	5.70	0.80
	52.42	52	−0.42	0.40	5.70	2.28
	52.42	53	0.58	0.37	5.70	2.11
	52.42	54	1.58	0.09	5.70	0.51
135	52.80	51	−1.80	0.05	5.49	0.28
	52.80	52	−0.80	0.30	5.49	1.68
	52.80	53	0.20	0.45	5.49	2.52
	52.80	54	1.20	0.18	5.49	1.01
136	53.15	51	−2.15	0.008	5.26	0.04
	53.15	52	−1.15	0.20	5.26	1.11
	53.15	53	−0.15	0.45	5.26	2.50
	53.15	54	0.85	0.29	5.26	1.61

[a] See Ref. 14.

Pappas[14] has suggested a modification of the equal charge displacement hypothesis by proposing that equal charge displacement applies before neutron emission. Independent yields are calculated by his method in the following manner: First, Z_p is calculated by

$$Z_p=Z_{A+n}-\tfrac{1}{2}(Z_{238-A-n}+Z_{A+n}-92). \quad (3)$$

The most probable charges, Z_{A+n} and $Z_{238-A-n}$, are obtained from the maximum stability lines of Coryell.[15] Secondly, the fractional yield is read from Fig. 4. The results of such calculations are shown in Table II. Finally, a correction for the emission of prompt shell neutrons is made.

The fission yields for $A=131$ to 135 may be obtained by summing the resulting independent yields. The values are plotted in Fig. 3.

The actual values of the calculated yields are subject to the large error in drawing a smooth curve through the experimental points; nevertheless, it seems significant that the calculated yields do show fine structure at mass 132 in the same manner as observed experimentally.

The shape of the mass-yield curve in the region $A=131$–136 obtained in this work is unique in that the maximum value seems to be located at $A=132$ rather than $A=133$, 134, or 136. Previously, two instances were known, where the maximum is located at $A=133$,

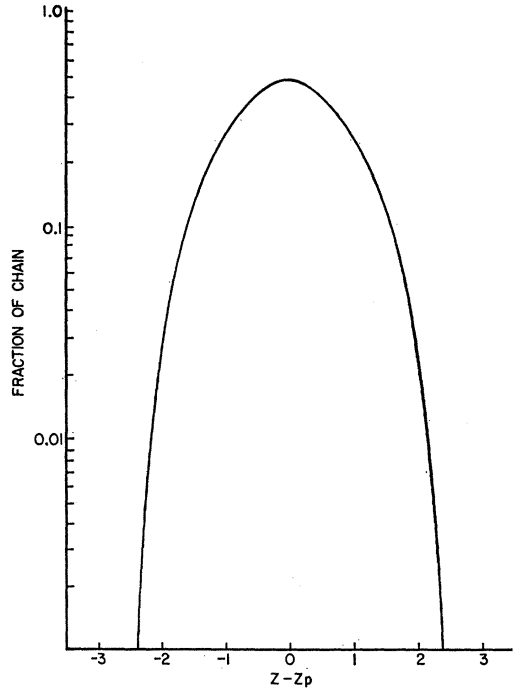

FIG. 4. Variation of yield with nuclear charge. Determined by G. P. Ford *et al.*, Los Alamos Scientific Laboratory Report No. LA-1997, 1956 (unpublished).

[14] A. C. Pappas, MIT Technical Report No. 63, 1953 (unpublished).

[15] C. D. Coryell, Ann. Rev. Nucl. Sci. **2**, 325 (1953).

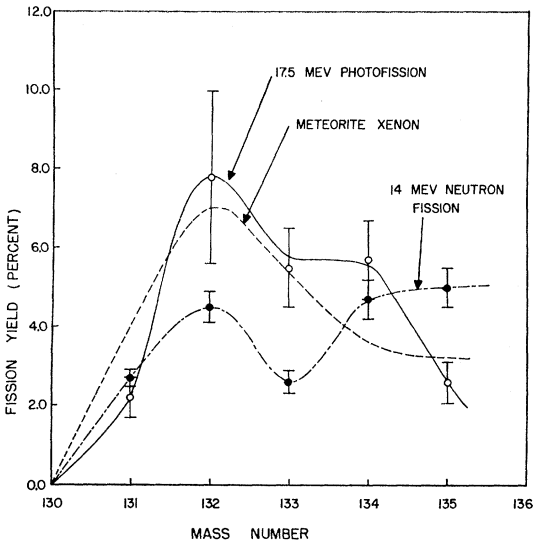

FIG. 5. Comparison of the abundance pattern of the excess "fissiogenic" xenon isotopes in the Fayetteville meteorite with the mass-yield curves from photofission and 14-MeV-neutron-induced fission of U^{238} reported by Broom (Ref. 12).

i.e., the spontaneous fission of Pu^{240} reported by Laidler *et al.*,[16] and the U^{238} photofission reported by Richter and Coryell.[2] In both of these cases, however, the mass-yield values for five consecutive mass numbers for $A=131$–135 have not been measured and hence the exact location of the maximum value is uncertain.

It is worthy of note, however, that the mass-yield values at $A=133$ are considerably higher than the values near $A=136$ in both cases. Manuel and Kuroda[17] have recently reported that there is an excess of fission-produced stable xenon isotopes in the light phase of the Fayetteville meteorite and also the Pantar meteorite, relative to the dark phase. The amount of excess fission xenon in the meteorites cannot be accounted for by the spontaneous fission of U^{238} alone. Moreover, a calculation based on the spontaneous fission decay of the extinct nuclide Pu^{244} does not seem to account for all the fission-produced xenon isotopes found in the meteorite. They suggested the possibility that part of the fission-produced xenon isotopes in the meteorite was produced by either the neutron-induced fission or photofission of uranium or thorium. The shapes of the mass-yield curves in this region for the neutron-induced fission of uranium and thorium, however, are quite different from the general shape of a plot of the abundance pattern of the fission-produced xenon isotopes in the meteorite, in which Δ_i values defined as follows are plotted against mass number i:

$$\Delta_i=[\mathrm{Xe}^i/\mathrm{Xe}^{130}]_L-[\mathrm{Xe}^i/\mathrm{Xe}^{130}]_D,$$

where the subscripts L and D refer to the light and dark phases of the meteorites. The plot of Δ_i values against mass number i has a maximum at $i=132$ and is very similar to the shape of the U^{238} photofission mass-yield curve in the region $A=131$–135, as shown in Fig. 5.

Although it is difficult to prove unequivocally at this time that we are observing the part of the photofission mass-yield curve of U^{238} in the abundance pattern of the stable meteoritic xenon isotopes, it is nevertheless of great interest to point out that the conditions under which the planetesimals were irradiated by solar protons during the synthesis of light elements in the early history of the solar system were probably such that the photofission process might have played an important role. According to Fowler *et al.*[18,19] and also Mitler,[20] the irradiation period may have lasted for 10^7 years and the neutron flux near the surface of the planetesimals could have been as high as 10^7 neutrons/cm^2 sec.

Assuming that the excess fission xenon was formed by the photofission of uranium, rather than the spontaneous fission of the extinct nuclide Pu^{244}, the necessary flux of gamma rays to produce the excess xenon can be calculated from

$$\begin{aligned}\Delta_i&=[\mathrm{Xe}^i/\mathrm{Xe}^{130}]_L-[\mathrm{Xe}^i/\mathrm{Xe}^{130}]_D\\&=([\mathrm{U}^{238}/\mathrm{Xe}^{130}]_L-[\mathrm{U}^{238}/\mathrm{Xe}^{130}]_D)e^{\lambda_{238}T}y_i\Delta t\Phi\sigma,\end{aligned}$$

where T ($=4.55\times10^9$ years) is the age of the meteorite, y_i is the fission yield for the chain i, Δt ($=10^7$ years) is the duration of the planetesimal irradiation period, Φ is the flux of gamma rays, and σ is the photofission cross section ($=5\times10^{-26}$ cm^2) for the uranium.

A value of $\Phi=5\times10^6$ γ/cm^2 sec is obtained from the above equation. This is somewhat lower than the neutron flux required in the irradiation model of Fowler *et al.*,[18] and the calculated gamma-ray flux seems to be not at all unreasonable.

ACKNOWLEDGMENTS

The authors would like to thank the U. S. Atomic Energy Commission for support of this work through the Contract No. At-(40-1)-3235. We are grateful to R. Ganapathy for allowing us to use some of his unpublished data.

[16] J. B. Laidler and F. Brown, J. Inorg. Nucl. Chem. **24**, 1485 (1962).
[17] O. K. Manuel and P. K. Kuroda, J. Geophys. Res. **69**, 1413 (1964).
[18] W. A. Fowler, J. L. Greenstein, and F. Hoyle, Geophys. J. Roy. Astron. Soc. **6**, 148 (1962).
[19] W. A. Fowler, Science **135**, 1037 (1962).
[20] H. E. Mitler, Phys. Rev. **136**, B298 (1964).